communications biology

A Nature Portfolio journal

Article

https://doi.org/10.1038/s42003-025-07718-4

The long noncoding RNA LUCAT1 regulates endometrial receptivity via the miR-495-3p/S100P axis

Junyu Shang[1,2,3], Yumei Chen[2,4], Qianwen Jiang[5], Wenxin Li[1,2,3], Minjun Lu[1,2,3], Jiamin Zhou[1,2,3], Li Lin[1,2,3], Jie Xing[1,2,3], Mengxue Zhang[1,2,3], Shijie Zhao[1,2,3], Jingjing Lu[1,2,3], Xuyan Shi[1,2,3], Yueqin Liu[1,2,3] & Xiaolan Zhu[1,2,3] ✉

Recently, interest in investigating the effects of long noncoding RNAs (lncRNAs) on endometrial receptivity (ER) has increased within the field of assisted reproductive technology. Therefore, the objective of this study is to identify and analyze the role of the lncRNA LUCAT1 and to elucidate its specific mechanism in regulating ER. Hub genes associated with ER are identified via Weighted gene co-expression network analysis (WGCNA) in two datasets downloaded from the GEO database. These hub genes identified via WGCNA were subsequently validated. The combination of a dual-luciferase assay, qRT–PCR, western blotting, and other techniques are used to investigate the molecular mechanism by which LUCAT1 regulates S100P. In this study, LUCAT1 expression is shown to significantly affect ER, and the depletion of LUCAT1 leads to impaired ER function. Additionally, LUCAT1 is shown to act as a molecular sponge for miR-495-3p, thereby modulating the expression of S100P. This modulation influences the proliferation, migration, and invasion capabilities of Ishikawa cells, as well as the adhesion of JAR cells to endometrial cells. Therefore, LUCAT1 can regulate ER via the miR-495-3p/S100P axis, which provides experimental evidence for the identification of innovative strategies aimed at enhancing endometrial receptivity.

In recent decades, the success rate of in vitro fertilization–embryo transfer (IVF-ET) has significantly improved due to advancements in embryo laboratory technology and clinical techniques. However, approximately 50% to 60% of IVF-ET cycles do not result in successful implantation[1]. Endometrial receptivity (ER) and embryo quality are pivotal factors contributing to implantation failure[2]. Recurrent implantation failure (RIF), defined as the inability to achieve a clinical pregnancy after at least three or more high-quality embryos are transferred during fresh or frozen cycles before the age of 40[3], represents a significant limitation to the success rates of IVF-ET and implantation. The prevailing belief is that aberrant ER functions as the primary determinant of RIF. Enhancing ER functionality holds potential for mitigating the reduced implantation potential and facilitating higher rates of successful implantation. Therefore, numerous scholars have suggested that an accurate evaluation and enhancement of ER may represent key breakthroughs to improve the outcomes of IVF-ET and implantation[4].

ER is the ability of the endometrium to support successful embryo implantation and serves as a crucial determinant for achieving a normal pregnancy. ER encompasses a specific timeframe during the mid-secretory stage known as the window of implantation (WOI), which is characterized by the optimal uterine morphology and functionality, facilitating blastocyst adhesion and subsequent implantation[5]. Researchers in the field of assisted reproductive technology have been striving to establish a universally accepted benchmark for evaluating ER, yet a consensus remains elusive. Numerous conventional methodologies are available for evaluating ER. Ultrasonic detection is a widely employed diagnostic tool in clinical practice that enables the assessment of various parameters, such as endometrial volume, blood flow dynamics, thickness, and histologic characteristics[6]. This method is cost-effective and noninvasive, which makes it widely accepted. However, the lack of consensus on standards for ultrasonic detection, such as endometrial thickness and vascularization, has led to ongoing controversy surrounding its predictive value in determining pregnancy outcomes[7]. Additionally, histologic techniques can provide a more precise evaluation of endometrial differentiation and maturation. However, their invasive nature may not be well received by patients. The endometrial

[1]Reproductive Medicine Center, The Fourth Affiliated Hospital of Jiangsu University, Zhenjiang, China. [2]Department of Central Laboratory, The Fourth Affiliated Hospital of Jiangsu University, Zhenjiang, China. [3]Reproductive Sciences Institute, Jiangsu University, Zhenjiang, China. [4]The Department of Gynecology, the Fourth Affiliated Hospital of Jiangsu University, Zhenjiang, China. [5]College of Pharmacy, Guangxi University, Nanning, China. ✉e-mail: zxl2517@163.com

receptivity array (ERA), which is based on an analysis of 238 genes believed to be involved in ER, represents an endeavor to improve histologic detection from a clinical perspective. However, the current published data supporting the ERA are limited and await the results of an international, randomized, multicenter trial[8]. More significantly, the exorbitant cost associated with a single ERA examination renders it financially unfeasible for patients, thereby impeding its widespread clinical implementation. Recently, been rapid development of second-generation sequencing technology, particularly RNA sequencing (RNA-seq), has occurred. Transcriptomic studies have emerged as powerful tools for comprehensively assessing alterations in gene expression, playing crucial roles in disease research, diagnosis, and treatment. Several commonly accepted markers of ER, including S100P[9], LIF[10], COX-2[11], HOXA10[12], VEGF[13] and β3 integrin[14], have been proposed. However, the clinical applications of these proteins and relevant technologies are still in the early stages. Therefore, the diligent identification and validation of objective, precise, and distinctive markers linked to ER are imperative.

Long noncoding RNAs (lncRNAs) are RNA molecules that exceed a transcript length of 200 nucleotides and do not encode proteins[15]. LncRNAs have gained significant recognition for their diverse functional roles in various biological processes within the endometrium. Several lncRNAs, including CASC2, LINC00672, TUG1, and TUSC7, exert tumor-suppressive effects on endometrial cancer and enhance tumor chemosensitivity[16]. Furthermore, several lncRNAs are involved in evaluating ER. H19 has been found to be downregulated in the endometria of patients with RIF[17]. Compared with the levels in pregnant individuals, AK124742 and PSMD6 were downregulated in cumulus cells in non-pregnant individuals[18]. Wang et al. identified a novel candidate gene, TUNAR (lnc00617), and employed it as a molecular marker for ER by comparing the transcriptional sequencing data of LH + 2 and LH + 7 in the human endometrium through RNA-seq analysis[19]. The above studies indicate that these lncRNAs are strongly correlated with and are predictive of ER, but their specific underlying mechanisms need to be further explored. Therefore, we attempted to identify additional ER markers among the identified lncRNAs. The GSE106602 and GSE98386 datasets uploaded by Suhorutshenko M et al. contain the differential gene expression profiles of early secretory- and mid-secretory-phase endometrial biopsies obtained from 70 healthy fertile women across one menstrual cycle[20]. Weighted gene co-expression network analysis (WGCNA) was used to construct a lncRNA–mRNA coexpression network for ER and to screen for hub genes. The highly connected protein-coding gene S100P and the lncRNA LUCAT1 were selected. Given the inaugural investigation of LUCAT1 in the endometrium, our findings reveal its multifaceted functions within this tissue. LUCAT1 not only influences embryo adhesion to the epithelium but also governs the decidualization processes of endometrial stromal cells (ESCs). Our study substantiates the indispensable role played by LUCAT1 in facilitating embryo implantation and potentially provides a promising biomarker for assessing ER.

Results

The lncRNA LUCAT1 and S100P are hub genes in the RNA–RNA network related to ER

Seventy endometrial samples from two endometrial sample sequencing datasets (GSE106602 and GSE98386) in the GEO database were analyzed via WGCNA to explore the marker molecules associated with ER (Fig. S1A). The gene distributions in the early secretory-stage (LH + 2) and middle secretory-stage (LH + 7 for samples from Spain and LH + 8 for samples from Estonia) samples are shown in cluster diagrams (Fig. 1A). After the soft threshold was set to 10 (Fig. S1B), the genes were divided into different modules, which were indicated with 15 different colors (Fig. S1C), for further analysis. The mRNAs and lncRNAs exhibiting similar expression patterns were grouped into modules using average-link clustering (Fig. 1B up). In addition, an eigengene adjacency heatmap displayed the correlations between gene modules (Fig. 1B down). The module trait relationships are shown in the heatmap (Fig. 1C). The turquoise module, which presented the most significant discrepancy between LH + 2 and LH + 7 or LH + 8 among the 15 modules, was selected as the significant module for further analysis. The mRNAs in the turquoise module were subjected to GO analysis and KEGG pathway enrichment analysis. The GO analysis revealed that these mRNAs were enriched in signal transduction, extracellular matrix organization, neutrophil degranulation and angiogenesis (Fig. 1D). The KEGG pathway enrichment analysis suggested that metabolic pathways and pathways in cancer were the most significantly enriched pathways (Fig. 1E). The genes in the turquoise group were related mainly to signal transduction, according to the heatmap of the GO (Gene Ontology) analysis. Based on the WGCNA results, 22 lncRNAs and 48 mRNAs constituted the lncRNA–mRNA co-expression network (Fig. 1F). In the network, a classical ER molecule, S100P, was shown to be a hub gene, and the lncRNA LUCAT1 was connected to S100P. The results of the WGCNA and co-expression network analysis indicated that S100P and LUCAT1 might be associated with ER.

LncLUCAT1 and S100P are upregulated in receptive endometrial cells

We initially confirmed the expression of LUCAT and S100P in endometrial tissue to analyze the relationships among lncLUCAT1, S100P and ER. Endometrial tissue was isolated from early secretory-stage and middle secretory-stage samples. Compared with the levels in early secretory-stage endometrial tissue, LUCAT1 and S100P were upregulated in middle secretory-stage endometrial tissue (Fig. 2A, B). IHC revealed the same pattern of S100P expression (Fig. S2C). Furthermore, typical multi-fluorescence images showed the colocalization of S100P, Ki67 and CK7 in endometrial epithelial cells, indicating the involvement of S100P in glandular formation. In the LH + 7 group, increased expression of S100P was observed in a greater number of glandular cells formed vesicles, consistent with previous experimental findings (Fig. 2A).

The same results were obtained for Ishikawa cells, a well-differentiated endometrial adenocarcinoma cell line. The principal hormones regulating uterine function, E2 and P4, were added to Ishikawa cells, which were subsequently induced to enter the receptive stage. This induction was characterized by elevated levels of the HOXA10 and β3 integrin markers (Fig. S2B, C). In Ishikawa cells, low concentrations of E2 promoted the expression of LUCAT1 but high concentrations inhibited its expression (Fig. 2D), whereas P4 promoted LUCAT1 expression in a concentration-dependent manner (Fig. 2E). When P4 (0.1 μM) and E2 (0.01 μM) were added together (at the physiological concentrations of the middle secretory stage), LUCAT1 expression was significantly upregulated (Fig. 2F). Similar to LUCAT1 expression, the S100P mRNA and protein levels were regulated by E2 and P4 (Fig. 2G, H). As expected, the expression of NF-κB p65, a marker molecule of the NF-κB signaling pathway that is regulated by S100P, was upregulated in Ishikawa cells treated with E2 and P4 (Fig. 2H). In summary, LUCAT1 and S100P are upregulated in middle secretory-stage endometrial cells.

LUCAT1 depletion impairs the ER of endometrial cells

Based on the expression pattern of LUCAT1, we evaluated whether LUCAT1 regulates the ER of Ishikawa cells by performing functional experiments with LUCAT1-silenced Ishikawa cells. The proven LUCAT1 silencing (Fig. S3A) inhibited the proliferation (Fig. 3A), migration (Fig. 3B), and invasion (Fig. 3C) of Ishikawa cells, which indicated that LUCAT1 knockdown affected ER. We further elucidated the involvement of LUCAT1 in ER by next performing an attachment assay to assess whether LUCAT1 affects blastocyst attachment to the endometrium. JAR spheroids (Fig. 3D, top panel) served as embryonic bodies and were added to a single layer of Ishikawa cells and incubated for 1 h (Fig. 3D, bottom panel). After washes with PBS, a significantly greater number of JAR spheroids remained on LH + 7 Ishikawa cells than on control cells, but the number was reduced by LUCAT1 silencing (Fig. 3D, right panel), suggesting that LUCAT1 plays an indispensable role in regulating ER.

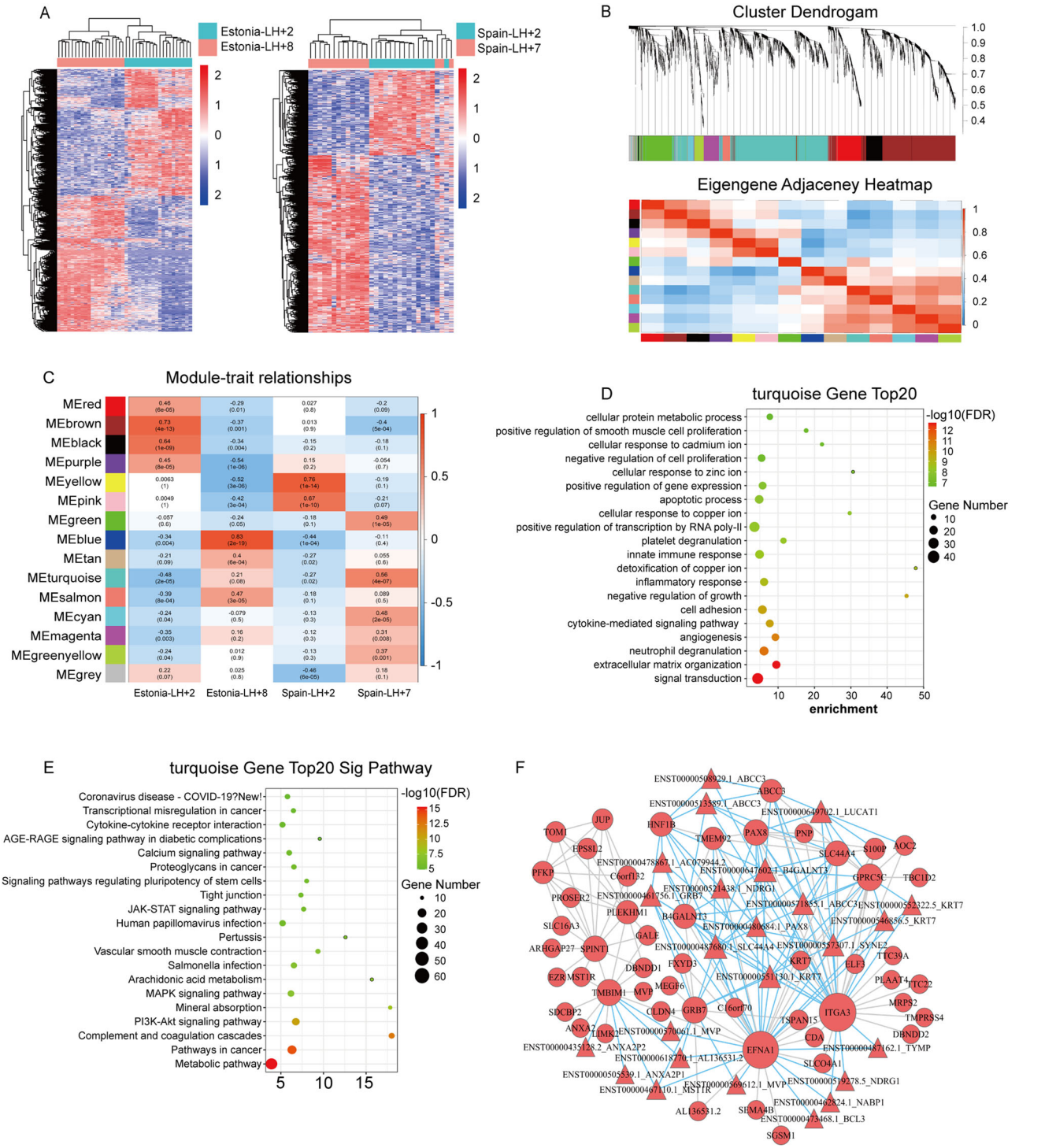

Fig. 1 | Analyze data sets and screen hub genes. A Heatmaps depicting the differential expression of RNAs between LH + 2 and LH + 7 for samples from Spain or LH + 8 for samples from Estonia generated using microarray data from two independent studies (left panel: GSE106602, right panel: GSE98386). **B** Clustering dendrogram of genes, utilizing dissimilarity derived based on topological overlap (up), and heat map of gene eigengene adjacency, displaying assigned module colors (down). **C** Heatmaps illustrating the correlation between eigengene and clinical traits of genes. Each row corresponds to a module eigengene. Each cell contains the corresponding correlation and p-value. **D** Gene Ontology analysis of the turquoise module. **E** Pathway analysis of the turquoise module. **F** The network of the top hub genes in the turquoise module.

In addition to the attachment assay, we explored the expression of LUCAT1 during decidualization. The isolated human primary ESCs (Fig. 3E) were identified using vimentin (a marker of stroma cells). ESC decidualization was induced by the addition of MPA and cAMP for 0, 2, 4, or 6 consecutive days. Subsequently, time-dependent increases in the levels of decidualization markers, including insulin-like growth factor-binding protein 1 (IGFBP1) and prolactin (PRL), were observed (Fig. 3F, G). In response to decidualization stimulation, the expression of LUCAT1 increased significantly (Fig. 3H). Notably, the knockdown of LUCAT1 significantly attenuated this increase (Fig. 3I, J). In summary, the above results suggest that LUCAT1 depletion impairs the receptivity of endometrial and Ishikawa cells.

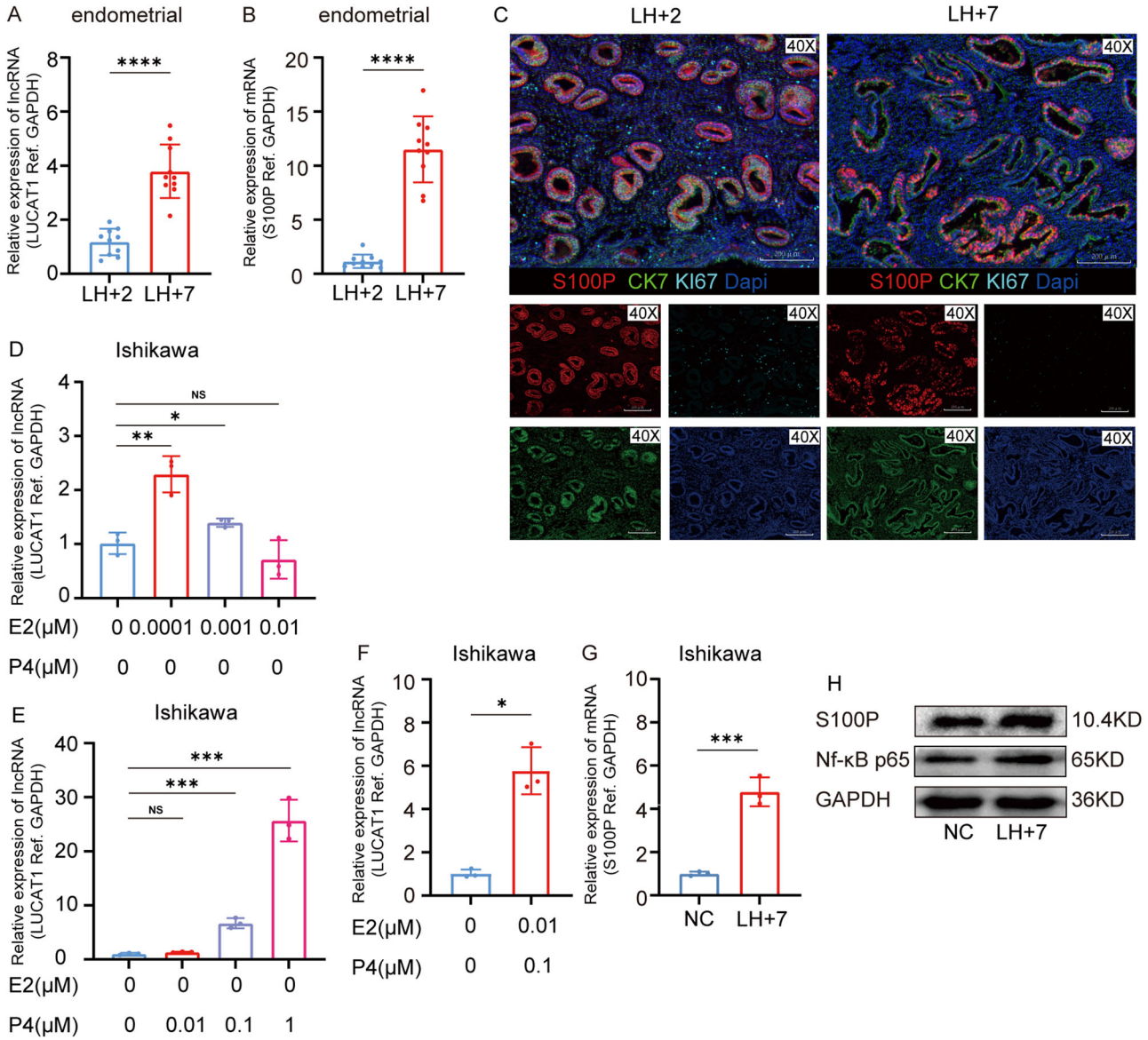

Fig. 2 | LUCAT1 and S100P are upregulated in LH + 7 endometrial cells relative to LH + 2 cells. A The relative expression of LUCTA1 in endometrial tissue ($n = 10$). **B** The relative expression of S100P mRNA in endometrial tissue ($n = 10$). **C** The distribution of CK7, KI67 and S100P in endometrial tissue showed by multiple fluorescence. **D** The effects of E2 on the expression of LUCAT1 in Ishikawa cells ($n = 3$). **E** The effects of P4 on the expression of LUCAT1 in Ishikawa cells ($n = 3$). **F** The effects of E2 and P4 on the expression of LUCAT1 in Ishikawa cells ($n = 3$). **G** The expression of S100P mRNA in Ishikawa cells ($n = 3$). **H** The expression of S100P and NF-κB p65 protein in Ishikawa cells. $^{*}P < 0.05$, $^{**}P < 0.01$, $^{***}P < 0.001$, and $^{****}P < 0.0001$. (Error bar: mean with SD.).

LUCAT1 regulates S100P signaling by sponging miR-495-3p

Based on the aforementioned findings, we aimed to elucidate the regulatory mechanism of LUCAT1 in relation to ER. First, we sought to validate the interaction network between LUCAT1 and S100P, and qRT-PCR and WB demonstrated that LUCAT1 knockdown resulted in a significant decrease in the expression level of S100P in Ishikawa cells (Fig. 4A, B). LncRNAs can serve as miRNA sponges to regulate cellular functions, which is a classical regulatory mechanism of lncRNAs. We explored whether LUCAT1 exerts its biological functions by sponging miRNAs. Using starBase, 17 miRNAs were found to have binding sites for LUCAT1, and 22 miRNAs had binding sites for S100P (Fig. S4A). However, only one miRNA (miR-495-3p) had binding sites for both S100P and LUCAT1 (Fig. 4C). A pulldown assay (Fig. 4D) using a biotinylated miR-495-3p probe showed the significant enrichment of LUCAT1 and S100P in the RNA pools pulled down by miR-495-3p (Fig. 4E, F). Furthermore, we performed a luciferase reporter assay and found that a miR-495-3p mimic obviously inhibited the luciferase activity of S100P-WT cells but had no influence on that of S100P-MUT cells (Fig. 4G, H).

In contrast to the upregulation of LUCAT1 and S100P, miR-495-3p was downregulated in middle secretory-stage endometrial cells (Fig. 4I). Similarly, miR-495-3p was downregulated by E2 and P4 in Ishikawa cells (Fig. 4J). In Ishikawa cells, LUCAT1 silencing upregulated the level of miR-495-3p (Fig. 4K). Furthermore, we found that miR-495-3p regulated the expression of S100P in Ishikawa cells. MiR-495-3p inhibitor upregulated the expression of S100P when LUCAT1 was knocked down (Fig. 4L). However, miR-495-3p inhibitor increased the expression of S100P in Ishikawa cells when S100P was silenced (Fig. 4M). Similarly, the expression of NF-κB p65 was consistent with that of S100P (Fig. 4M). Furthermore, the markers of ER, including β3 integrin, LIF, and HOXA10, did not show significant effects from this pathway (Fig. S4C, D, E), but the expression pattern of MMP9 was consistent with S100P (Fig. S4F). In summary, LUCAT1 regulates the level of S100P signaling by sponging miR-495-3p.

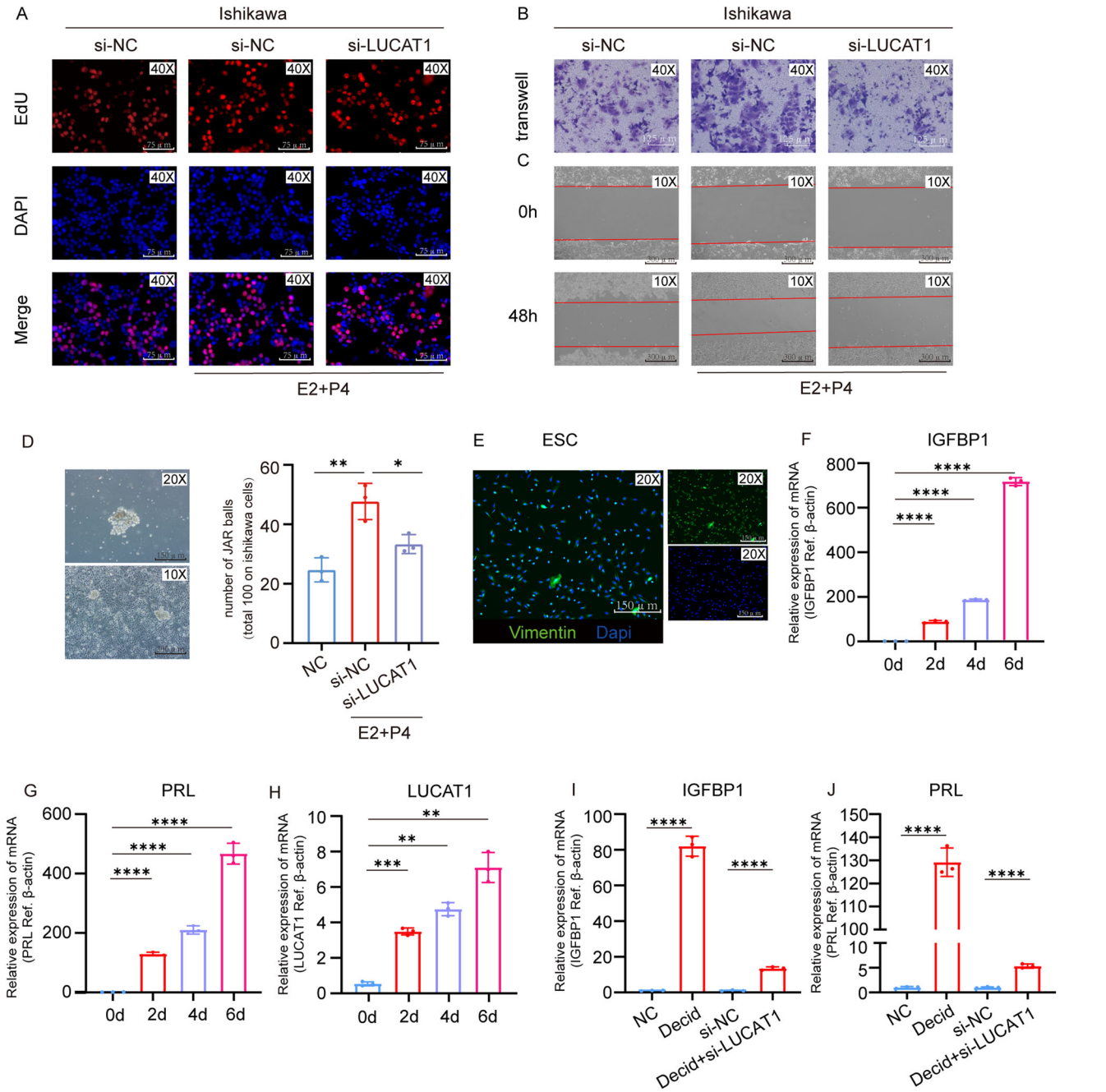

Fig. 3 | LUCAT1 is involved in establishing endometrial receptivity. A–C The effects of E2 + P4 and LUCAT1 silencing on the proliferation (**A**), invasion (**B**), migration (**C**) of Ishikawa cells ($n = 3$). **D** The effects of E2 + P4 and LUCAT1 silencing on blastocyst attachment to the endometrium ($n = 3$). **E** Immunofluorescence staining of vimentin (green) in ESCs and the nuclear were stained with DAPI (blue). **F**, **G** The expression of the markers of decidualization, IGFBP1 and PRL, in the ESCs induced by hormone ($n = 3$). **H** The expression of LUCAT1 during decidualization process ($n = 3$). **I**, **J** The effects of LUCAT1 silencing on the expression of IGFBP1 and PRL ($n = 3$). $^{*}P < 0.05$, $^{**}P < 0.01$, $^{***}P < 0.001$, and $^{****}P < 0.0001$. (Error bar: mean with SD.).

LUCAT1 regulates ER via the miR-495-3p/S100P axis

After confirming the involvement of the LUCAT1/miR-495-3p/S100P axis in Ishikawa cells, we further investigated its relationship with ER. Silencing of LUCAT1 inhibited the proliferation (Fig. 5A, Fig. S5A), migration (Fig. 5B, Fig. S5B), and invasion (Fig. 5C, Fig. S5C) abilities of Ishikawa cells, whereas these effects were reversed upon cell transfection with the miR-495-3p inhibitor (Fig. 5A, B, C, Fig. S5A, B, C). These findings suggest that LUCAT1 modulates ER through the regulation of miR-495-3p/S100P axis activity. The results of the adhesion assay between JAR and Ishikawa cells confirmed this conclusion, as fewer JAR spheroids adhered to Ishikawa cells following LUCAT1 knockdown, whereas the transfection of Ishikawa cells with the miR-495-3p inhibitor resulted in an increased number of adhered JAR spheroids (Fig. 5D). Thus, the LUCAT1/miR-495-3p/S100P axis plays a regulatory role in ER processes.

Inhibition of S100P attenuates ER and embryo implantation in vivo

A solution containing 1 μg of si-S100P was injected into the right horn of the mouse uterus, while si-NC was injected into the left horn as a control on Day 3 of pregnancy to further verify the roles of S100P in ER and embryo implantation in vivo (Fig. 6A). As a result, S100P silencing significantly

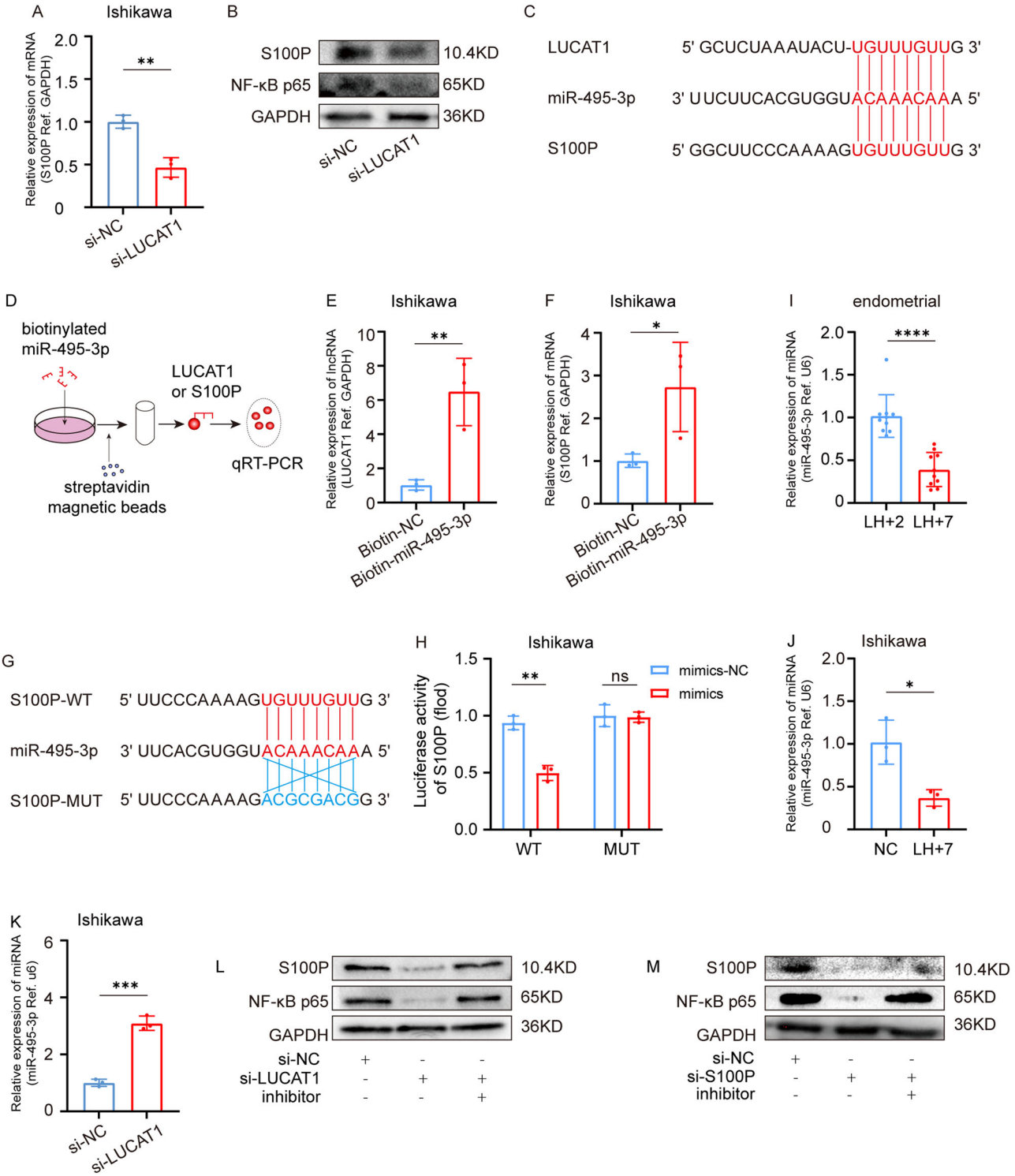

Fig. 4 | LUCAT1 regulates S100P signaling. A The relative expression of the mRNA of S100P affected by LUCAT1 silencing ($n = 3$). **B** The expression of S100P and NF-κB p65 protein affected by LUCAT1 silencing. **C** Predicting potential target microRNA of LUCAT1 and S100P, with complementary binding dot. **D** The schematic view of RNA-RNA pull down. **E** The relative expression of LUCAT1 in biotin-labeled adsorption assays ($n = 3$). **F** The relative expression of S100P in biotin-labeled adsorption assays ($n = 3$). **G** The changes of the dots of S100P-MUT. **H** Dual luciferase reporter assays about investigating the interaction between miR-495-3p and S00P 3′-UTR ($n = 3$). **I** The relative expression of miR-495-3p in endometrial tissue ($n = 10$). **J** The relative expression of miR-495-3p in Ishikawa cells ($n = 3$). **K** The relative expression of miR-495-3p affected by LUCAT1 silencing ($n = 3$). **L** The expression of S100P and NF-κB p65 protein in Ishikawa cells affected by LUCAT1 silencing or miR-495-3p inhibitor. **M** The expression of S100P and NF-κB p65 protein in Ishikawa cells affected by S100P silencing or miR-495-3p inhibitor. $^{*}P < 0.05$, $^{**}P < 0.01$, $^{***}P < 0.001$, and $^{****}P < 0.0001$. (Error bar: mean with SD.).

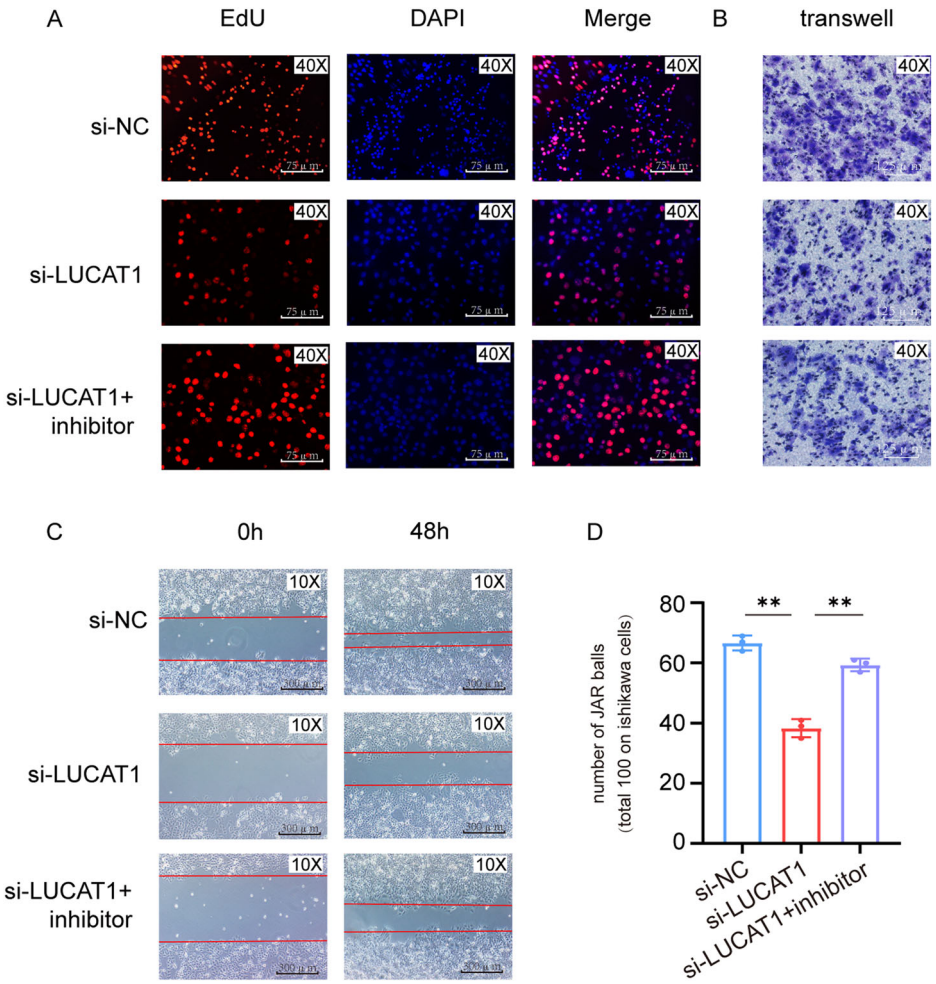

Fig. 5 | LUCAT1 regulates ER via the miR-495-3p/S100P axis. A–C The effects of LUCAT1 silencing or miR-495-3p inhibitor on the proliferation (**A**), invasion (**B**), migration (**C**) of Ishikawa cells ($n = 3$). **D** The effects of LUCAT1 silencing or miR-495-3p inhibitor on blastocyst attachment to the endometrium ($n = 3$). *$P < 0.05$, **$P < 0.01$, ***$P < 0.001$, and ****$P < 0.0001$. (Error bar: mean with SD.).

decreased the embryo implantation rate in mice that were dissected on Day 7 of pregnancy (Fig. 6B, C). However, the differences in embryonic development were not statistically significant (Fig. 6D). In tissue staining, S100P silencing downregulated the expression of S100P (Fig. 6E) in the uterine horn. H&E staining revealed decreased gland formation, and Ki67 staining revealed decreased endometrial proliferation in the si-S100P group (Fig. 6F, G). These results suggest that S100P may be involved in the regulation of ER and embryo implantation.

Discussion

The reported prevalence of endometrial factors contributing to two-thirds of IVF-ET failures underscores the increasing importance of ER in light of current high-quality embryo screening protocols[6]. The lack of ER is a pivotal barrier to advancing assisted reproductive technology. An accurate evaluation and enhancement of ER may be key for improving the success rate of IVF-ET. Despite the potential significance of lncRNAs, their functional roles and underlying molecular regulatory mechanisms remain largely unexplored. Moreover, few studies have investigated the relationship between noncoding RNAs and ER, resulting in numerous unknown areas that warrant further investigation. In this study, a lncRNA–mRNA co-expression network of hub genes in key module was constructed through WGCNA. The key module encompassed the majority of the genes related to ER that have been reported in previous studies, such as *ANXA2*, *GADD45A* and *MAOA*. The highly connected hub gene lncRNA LUCAT1 in this network attracted our interest. The newly discovered lncRNA LUCAT1 has been implicated in smoking-related lung cancer and is associated with an unfavorable prognosis for patients with smoking-related non-small cell lung cancer[21]. Recently, LUCAT1 has been associated with a broader spectrum of malignancies, including gastric[22], hepatic[23] and colorectal[24] carcinomas. The S100P protein, a member of the S100 family, plays a crucial role in regulating signaling pathways, protein phosphorylation, and cell proliferation and differentiation[25]. In studies pertaining to ER, S100P has been found to be significantly upregulated during the middle secretory stage, and S100P knockdown could induce apoptosis in endometrial epithelial cells[9], which aligns with the results of our bioinformatics analysis. LUCAT1 and S100P exhibit comparable characteristics in tumors and demonstrate strong associations within lncRNA–mRNA networks, which motivated us to conduct further investigations. In our study, we aimed to investigate the regulatory effect of LUCAT1 on ER through its ability to regulate S100P expression. qRT-PCR analysis revealed the upregulation of LUCAT1 in endometrial tissue during the middle secretory stage, which was consistent with the results of the bioinformatics analysis. Moreover, we hypothesized that the increased expression of LUCAT1 during this period might be associated with the establishment of the WOI. We subsequently conducted in vitro experiments using Ishikawa cells, an endometrial adenoma cell line, to examine the expression levels of LUCAT1. Interestingly, our results revealed a significant increase in LUCAT1 expression in cells treated with physiological concentrations of estrogen. After LUCAT1 RNA interference, the process of blastocyst attachment to the endometrium was hindered. Our findings unequivocally confirmed that targeted silencing of LUCAT1 resulted in a significant reduction in S100P expression. Numerous previous studies have consistently reported the involvement of LUCAT1 in the pathogenesis and metastasis of diverse malignancies, whereas recent investigations have revealed its participation in normal physiological processes.

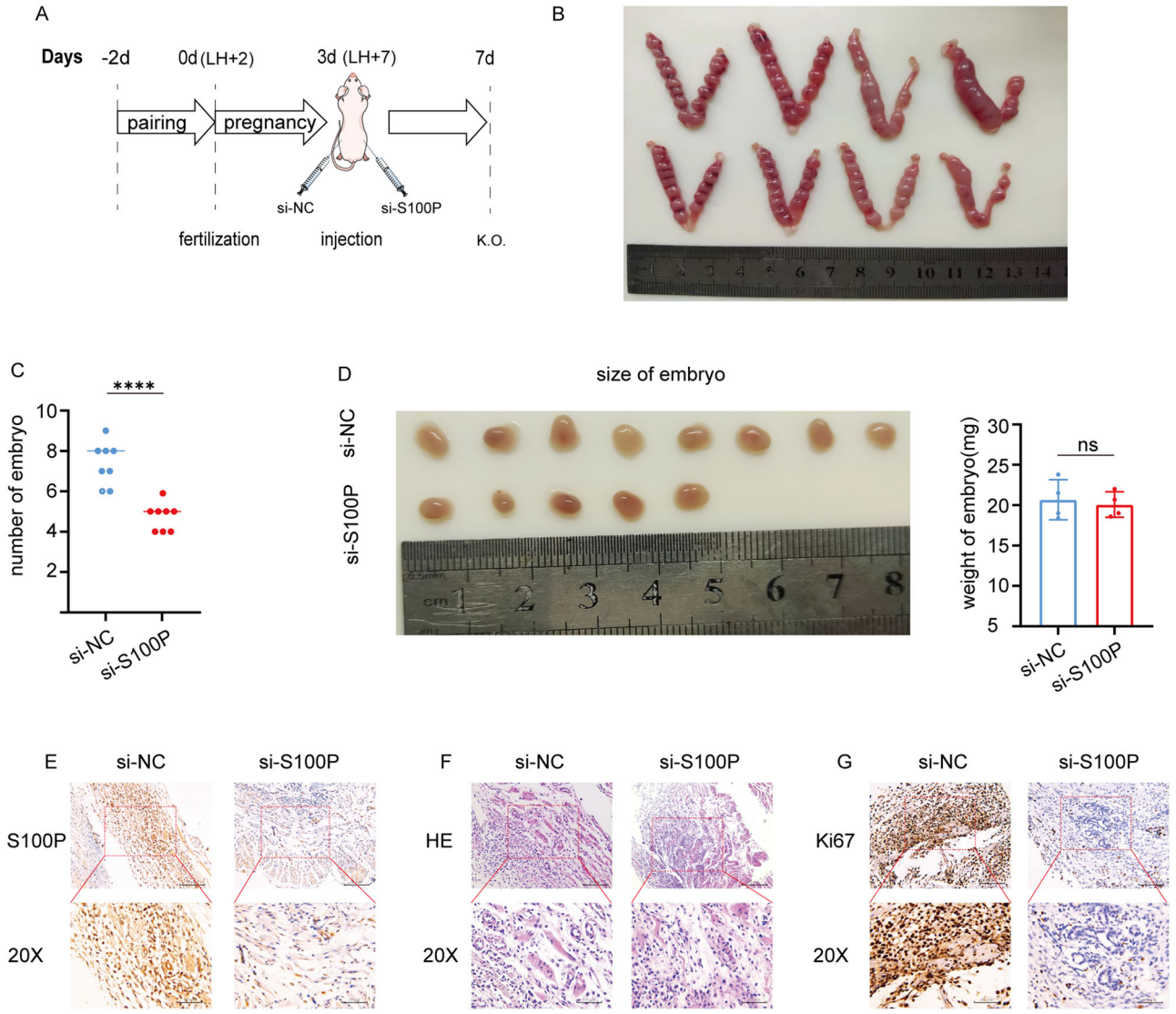

Fig. 6 | S100P affects endometrial receptivity and embryo implantation showed by an in vivo mouse model. A The process of the in vivo mouse model. **B**, **C** The number of embryo in the horn of mouse uterus with PBS or S100P silencing ($n = 8$). **D** The size and weight of embryo with si-NC or si-S100P ($n = 4$). **E** The expression of S100P in endometrium with si-NC or si-S100P. **F** The HE dye of endometrium with PBS or S100P silencing. **G** The Ki67 dye of endometrium with PBS or S100P silencing. $^{*}P < 0.05$, $^{**}P < 0.01$, $^{***}P < 0.001$, and $^{****}P < 0.0001$. (Error bar: mean with SD.).

Tao Y et al. reported that LUCAT1 knockdown increased the degree of MSC apoptosis and impaired MSC-mediated cardioprotection[26]. Our study is the first to identify a role for LUCAT1 in the reproductive system, especially in ER. The potential of LUCAT1 as a novel indicator for evaluating ER is predicted, and enhancing ER may be possible through LUCAT1 interventions.

Previous studies have shown the consistent upregulation of LUCAT1 in various cancer cell types[22–24]. Furthermore, LUCAT1 exerts its regulatory effect on tumor cells predominantly through the ceRNA network, modulating cell proliferation, migration, and invasion, which are key processes in tumorigenesis. The regulation of PTBP1 expression by LUCAT1 can modulate the drug resistance of tumor cells[27]. LUCAT1 functions as a competitive endogenous RNA (ceRNA) for miR-539, promoting cell proliferation, cell cycle progression, migration, and invasion of pancreatic ductal adenocarcinoma (PDAC)[28]. In fact, extensive similarities have been noted between tumor metastasis and embryo implantation, such as migration, invasion, and immune escape[29]. Conventional tumor factors, such as HOXA10 and VEGF, have been shown to regulate ER during embryo implantation. In our study, wound healing, invasion, and EdU experiments revealed that downregulating the expression of LUCAT1 significantly impeded the proliferation, migration, and invasive potential of Ishikawa cells, which may serve as a pivotal determinant contributing to the decrease in ER.

StarBase was used to predict the potential binding of miRNAs to LUCAT1 and S100P, and miR-495-3p was subsequently identified as a molecule that simultaneously bound to both targets. MiR-495-3p has been shown to exert a negative regulatory effect on the proliferation, migration and invasion of various tumor cells. The expression of miR-495-3p was found to be significantly downregulated in glioblastoma tissues and exhibited a negative correlation with LGMNP1 expression. Moreover, the tumor-promoting effects resulting from the upregulation of LGMNP1 could be mitigated by the introduction of miR-495-3p mimics[30]. Ectopic expression of miRNA mimics in gastric cancer (GC) cells resulted in the suppression of ten epithelial–mesenchymal transition (EMT)-related genes by miR-495-3p, leading to the inhibition of tumor cell growth and proliferation through both caspase-dependent and caspase-independent mechanisms of cell death[31]. In our study, an RNA–RNA pulldown assay confirmed the specific binding interaction between miR-495-3p and LUCAT1, as well as S100P. A dual-luciferase reporter gene assay subsequently confirmed the regulatory role of miR-495-3p in modulating S100P expression. The functional

integrity of the LUCAT1/miR-495-3p/S100P axis and its ceRNA mechanism were validated through rescue experiments. Notably, the expression pattern of MMP9 was consistent with S100P, but not as significantly different, which may indicate specific alterations in ER or indicate an underlying mechanism that remains to be elucidated. The inhibition of miR-495-3p reversed the suppressive effects of LUCAT1 silencing on S100P expression and cell proliferation, migration, and invasion upon RNA interference with LUCAT1. Moreover, in an embryonic cell adhesion experiment, miR-495-3p hindered the adhesion of JAR cell spheres to Ishikawa cells. Collectively, these findings underscore the effect of LUCAT1 on increasing ER levels while highlighting the effect of miR-495-3p on decreasing ER. Traditionally, researchers have postulated that S100P modulates cell proliferation, migration, and invasion by regulating RAGE ligands via the NF-κB pathway, which was repeatedly mentioned in several manuscripts by Arumugam T[32,33]. Mercado-Pimentel ME[34] and Onyeagucha BC[35]. Although S100P is commonly recognized as a prototypical ER-related molecule, its regulation is limited to hormonal factors. Our study represents a pioneering effort in elucidating and substantiating the intricate associations between hormones and S100P. Therefore, we hypothesize that S100P potentially regulates ER through the NF-κB pathway, which is based on our observed changes in the levels of the NF-κB marker p65.

In summary, the present results show that the expression of LUCAT1 and S100P is upregulated in endometrial tissues and cells during the receptive phase (Fig. 7). As a molecular sponge for miR-495-3p, LUCAT1 competitively binds to miR-495-3p, thereby increasing the expression level of S100P through a ceRNA mechanism. This change leads to the increased proliferation, migration, and invasion abilities of Ishikawa cells, as well as to increased adhesion between Ishikawa cells and JAR cell spheres. Furthermore, this process facilitates an improvement in ER and promotes the embryo implantation process. Unlike the unpredictable consequences associated with direct regulation of the S100P protein, regulating LUCAT1 expression within a safe range may represent a safer approach. Furthermore, considering that IHC and multifluorescence techniques revealed the absence of S100P in ESCs, another mechanism may be responsible for the decidualization-inducing effect of LUCAT1, although further investigation is needed. Although the precise mechanism underlying the LUCAT1-mediated regulation of decidualization remains elusive and warrants further investigation, a novel regulatory pathway involving ER is proposed, emphasizing the potential utility of LUCAT1 as a biomarker. Our observations suggest that LUCAT1 could be a new therapeutic target for improving ER and increasing the success of pregnancy by IVF-ET, thereby reducing implantation failure rates in IVF-ET.

Materials and methods

WGCNA, establishment of a weighted co-expression network and screening of hub genes

In this study, HIST2 and Stringtie were utilized to analyze two secretory endometrial samples from the GEO database (GSE106602 and GSE98386). The original fast-q transcriptome sequencing data of 70 samples collected from 35 women (20 from Estonia and 15 from Spain) during the early and middle secretory phases were standardized and annotated. Standardized mRNA and lncRNA data were obtained after preprocessing the original sequencing data, followed by screening for differentially expressed mRNAs and lncRNAs using the R package DEseq2 ($p < 0.05$, padj <0.05, FC > 2).

WGCNA was conducted on the screened mRNAs and lncRNAs. Initially, based on the expression data for the mRNAs and lncRNAs included in this analysis, a soft threshold of 10 was determined. Using the established soft threshold, we subsequently constructed a weighted gene co-expression map and selected modules exhibiting optimal significance and differential expression during the early and middle secretory stages for subsequent GO analysis and pathway analysis. Hub genes, genes with high connectivity, are usually located upstream of networks, whereas genes with low connectivity are usually located downstream of networks (e.g., transporters and catalytic enzymes). Interactions between hub lncRNAs and hub mRNAs were identified by calculating the Pearson correlation coefficients of differentially expressed mRNAs and lncRNAs with a cutoff of |cor | > 0.5. The interactions were identified using a *p*.adjust value < 0.01. Furthermore, a lncRNA–mRNA network was constructed using Cytoscape software. Additionally, starBase was employed to predict potential miRNA binding sites within both the identified lncRNAs and mRNAs.

Patients and samples

A total of 20 patients with normal fertility (10 patients in the LH + 2 group and 10 patients in the LH + 7 group) were recruited from the Fourth Affiliated Hospital of Jiangsu University. The inclusion criteria were as follows: 1. Patients were aged younger than 40 years. 2. Women with normal fertility were those who had a history of successful pregnancies and were admitted to our hospital for open or hysteroscopic surgery due to benign reproductive system conditions (such as ovarian cysts and uterine fibroids). 3. All enrolled patients were excluded if they presented with acute inflammation of the reproductive system, malignant tumors, systemic diseases (e.g., hepatitis or thyroid disease), or endocrine disorders (e.g., polycystic ovary syndrome or diabetes).

Contraceptive drugs were not administered, and intrauterine contraceptive rings were not inserted for a period of 3 months prior to sampling. Endometrial samples were obtained through endometrial pipette aspiration, endometrial scratching, or hysteroscopic endometrial biopsy. The sample collection procedure was approved by the Ethics Committee of the Fourth Affiliated Hospital of Jiangsu University (2022006) and adhered to ethical requirements. All ethical regulations relevant to human research participants were followed. All the participants volunteered and provided written informed consent. Following sample collection, specimens from women with normal fertility were categorized into the LH + 2 group and LH + 7 group based on a pathologist's evaluation, which was consistent with the presumed menstrual cycle phase. All the samples were subsequently collected, grouped, and stored in a −80 °C freezer until further analysis according to standard protocols.

Cell lines and cell culture

Ishikawa cells (endometrial epithelial cancer cells that perform as endometrial epithelial cells) and JAR cells (trophoblastic tumor cells that perform as embryos) were purchased from iCell Bioscience, Inc. (Shanghai, China). The cells were identified by STR analysis. Ishikawa cells were cultured in phenol red-free DMEM (GIBCO, USA) supplemented with 10% FBS at 37 °C with 5% CO_2. JAR cells were cultured in phenol red-free RPMI 1640 (GIBCO, USA) supplemented with 10% FBS at 37 °C and 5% CO_2. Passaging was performed when cell growth and fusion reached 80 to 90%, typically resulting in two subsequent passages. The passage period usually lasted for 2 days.

Endometrial cells were enzymatically isolated from human endometrium curettage samples according to a selective attachment method, with minor modifications. All the endometrial samples were minced into small pieces (1 mm^3) and digested with 0.2% collagenase I (Sigma, USA) for 60 min at 37 °C, followed by digestion with 0.1% deoxyribonuclease I (Sigma, USA) for 20 min. Subsequently, the tissues were filtered through a 40-μm (pore size) mesh to separate the ESCs. ESCs were passed through two strainers and cultured in phenol red-free DMEM/F12 (GIBCO, USA) supplemented with 10% fetal bovine serum (FBS) (GIBCO, USA) at 37 °C with 5% CO_2. Passaging was performed when cell growth and fusion reached 80 to 90%, typically resulting in two subsequent passages. The passage period usually lasted for 4 days.

Treatment with estradiol (E2) and progesterone (P4)

The cells were plated in 6-well plates (5×10^5 cells/well) and cultured in phenol red-free DMEM (GIBCO, USA) supplemented with 10% FBS at 37 °C with 5% CO_2 for 24 h. After starvation in serum-free and phenol red-free DMEM for 24 h, the cells were treated with E2 (0.0001, 0.001, or 0.01 μM) and P4 (0.01, 0.1, or 1 μM) in phenol red-free DMEM supplemented with 10% charcoal-stripped FBS for 24 h. The same concentration

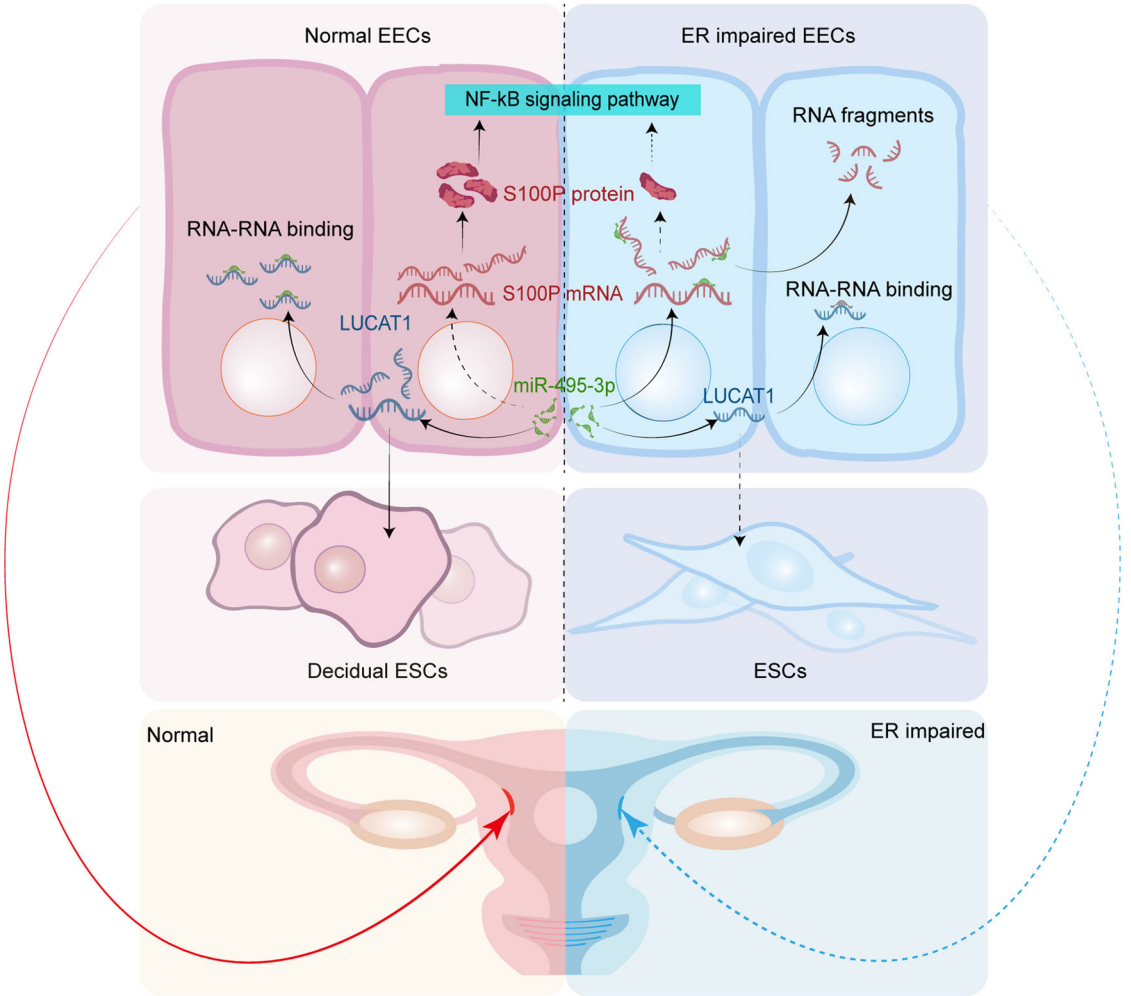

Fig. 7 | Schematic of the mechanisms involving LUCAT1 in the regulation of ER.

Table 1 | SiRNA and miRNA inhibitor sequences

Primer Name	Sense (5'-3')	Antisense (5'-3')
si-S100P	AAUGGAGAUGCCCAGGUGGACTT	GUCCACCUGGGCAUCUCCAUUTT
Si-NC	UUCUCCGAACGUGUCACGUTT	ACGUGACACGUUCGGAGAATT
miR-495-3p inhibitor	AAGAAGUGCACCAUGUUUGUUU	
miR-495-3p inhibitor NC	CAGUACUUUUGUGUAGUACAA	
si-LUCAT1	GCUCCUUUCCUCACAAGAATT	UUCUUGUGAGGAAAGGAGCTT

of dimethyl sulfoxide (DMSO) was administered to the control groups. Physiological concentrations of E2 (0.01 μM) and P4 (0.1 μM) were administered to the cells as the LH + 7 group.

Small interfering RNAs, miRNA inhibitors and transfection

Small interfering RNAs (siRNAs), control siRNAs (si-NCs), miRNA inhibitors and inhibitor-NCs were purchased from Gene Pharma, Shanghai, China. After being incubated with FBS-free culture medium, Ishikawa cells were transfected with 70 nM siRNAs or inhibitor per sample using Lipofectamine® 2000. The sequences of the siRNAs and inhibitors are shown in Table 1.

Quantitative real-time polymerase chain reaction (qRT–PCR) analysis

Total RNA was extracted from the tissues and cells using TRIzol reagent (Thermo, USA). In accordance with the instructions provided by the reagent manufacturer, 2 μg of total RNA was used for the synthesis of first-strand cDNA with HiScript II Q RT SuperMix (Vazyme, Nanjing, China) for mRNAs or an miRNA 1st Strand cDNA Synthesis Kit (Vazyme, Nanjing, China) for miRNAs. In addition, gDNA eraser was contained in the kits listed above. The stem-loop primer of miR-495-3p (GTCGTAAGTGCAGGGTCCGAGGTATTCGCACTGGATACGACAAGAAG) was added during the reverse transcription of miR-495-3p. The RNA level was measured via qPCR with ChamQ Universal SYBR qPCR Master Mix (Vazyme, Nanjing, China) on a real-time fluorescence quantitative PCR system (Bio-Rad, USA). The final concentration of each primer sequence was 10 mM. The reaction system was denatured at 95 °C for 30 sec (or 3 min for miR-495-3p), followed by 40 two-step cycles of 95 °C for 10 sec and 56 °C for 30 sec. The primers used in the study are shown in Table 2 or Table S1. GAPDH was used as a control for mRNAs or lncRNAs (β-actin served as the internal control in ESCs), and U6 was used as a control for miRNAs. Relative expression was determined after normalization to the

Table 2 | RNA primer sequences

Primer Name	Primer sequence (5'-3')
miR-495-3P F	ACGCTGAAAAACAAACATGGTG
miR-495-3P R	CAGTGCAGGGTCCGAGGT
LUCAT1-F	GACAATGCCCAGACCTCCAGAAAC
LUCAT1-R	GGAAAGGAGCCAGAAGTCAGAACAC
S100P-F	TACCAGGCTTCCTGCAGAGT
S100P-R	AGGGCATCATTTGAGTCCTG
IGFBP1-F	AGCACGGAGATAACTGAGGAGGAG
IGFBP1-R	GTTGGTGACATGGAGAGCCTTCG
PRL-F	GCAGATGGCTGATGAAGAGTCTCG
PRL-R	GGCTTAGCAGTTGTTGTTGTGGATG
GAPDH -F	CAGGAGGCATTG CTG ATGAT
GAPDH -R	GAAGGCTGG GGCTCATTT
miR-495-3P F	ACGCTGAAAAACAAACATGGTG
miR-495-3P R	CAGTGCAGGGTCCGAGGT
U6-F	CTCGCTTCGGCAGCACAT ATACT
U6-R	ACGCTTCACGAATTTGCGTGTC
β-actin-F	TGACGTGGACATCCGCAAAG
β-actin-R	CTGGAAGGTGGACAGCGAGG

GAPDH control or U6 control using the $2^{-\Delta\Delta Ct}$ method. All the experiments were repeated at least three times.

Western blot

Total protein was extracted using ice-cold radioimmunoprecipitation assay (RIPA) lysis buffer containing a phosphatase inhibitor and a protease inhibitor cocktail. After the proteins were separated on 10% SDS-PAGE gel, the wet transfer method was used to transfer the isolated proteins to a PVDF membrane at 200 mA for 2 h. After 2 h of blocking, the membrane was incubated overnight at 4 °C with antibodies against S100P (1:1000; Abcam, USA) or NF-κB p65 (1:1000; Abcam, USA). On the second day, the membrane was washed and then incubated with the appropriate secondary antibody conjugated to horseradish peroxidase for 1 h at room temperature. A G-Box iChemi chemiluminescence image capture system was used to visualize the bands. The same membrane was also probed with a GAPDH antibody (1:10,000; Proteintech, China) as an internal control. All the experiments were repeated at least three times.

Wound healing assay

When the transfected cells seeded in the 6-well plate reached confluence, scratches were made using a sterile 100 μl pipette tip. The cells were then incubated with FBS-free culture medium. Images of the scratches were captured at 48 h with an Olympus inverted microscope at 100× magnification. The width of the scratch was analyzed using Photoshop.

Matrigel invasion assay

Transwell migration assays were performed using transwell inserts with 8 μm pores. A total of 1×10^5 transfected cells were counted and seeded in the upper chamber of the insert (coated with 30 μl of Matrigel 6 h prior to seeding), while complete medium supplemented with 20% serum was added to the lower chamber. After 48 h of incubation, the cells were fixed with 4% paraformaldehyde and stained with a 0.1% crystal violet staining solution. The cells on the top surface of the membrane were wiped off, and the cells on the lower surface were examined with an Olympus inverted microscope at 100× magnification. The number of migrated cells was used as a measure of the migration capacity.

EdU cell proliferation assay

After Ishikawa cells were transfected with the siRNA or inhibitor plasmid for 24 h, EdU was added to the cells to a final concentration of 100 μM, and the cells were incubated for 2 h in an incubator at 37 °C with 5% CO_2. After the medium was removed, the cells were fixed with 4% paraformaldehyde for 15 min and then permeabilized with 0.4% Triton X-100. After washing, Apollo solution was added and incubated for 30 min to label the EdU-positive cells. The nuclei were counterstained with DAPI (blue). The stained sections were examined using a fluorescence microscope (Leica Microsystems, Mannheim, Germany).

In vitro embryo implantation

Ishikawa cells were seeded into 6-well plates at a density of 5×10^5 cells/well and incubated in phenol red-free DMEM supplemented with 10% FBS at 37 °C in a humidified incubator with 5% CO_2. After reaching 80% confluence, Ishikawa cells were transfected with si-NC or si-LUCAT1 using Lipofectamine® 2000. An attachment assay was conducted 48 h after transfection. JAR cells were seeded into 6-well plates at a density of 3×10^5 cells/well, incubated in RPMI 1640 supplemented with 10% FBS and 1% antibiotics for 24 h and shaken every half hour for the first 6 h at 37 °C in a humidified incubator with 5% CO_2. One hundred spheroids (50–100 μm in diameter) were transferred from each well onto the confluent monolayer of Ishikawa cells. After an incubation with the spheroids for 1 h, the attached spheroids were counted, and the attachment rate was reported as a percentage of the total number of spheroids (%).

Immunofluorescence staining

On the second day of culture, the cells in the chamber slide were fixed with 4% paraformaldehyde and permeabilized with 0.4% Triton X-100. After blocking, the cells were incubated with antibodies overnight at 4 °C. After washing, goat anti-rabbit immunoglobulin G (green) was used as a secondary antibody, and the cells were incubated in the dark for 1 h. The nuclei were stained with 4′,6′-diamino-2-phenylindole (DAPI) (1 mg/mL). Images were obtained with a microscope and camera connected to a computer with an image analysis system.

For multiple immunofluorescence staining, microwave treatment (for the elimination of the previous round of primary and secondary antibodies), blocking, primary antibody incubation, secondary antibody incubation, and signal amplification were conducted for different targets. Staining for S100P, KI67, CK7, and DAPI was performed, followed by the addition of drops of antifluorescence quenching sealing solution.

In vitro decidualization

ESCs were incubated with phenol red-free DMEM/F12 containing 2% stripped FBS, 5×10^{-4} M 8-Br dibutyryladenosine cAMP sodium salt (cAMP) and 10^{-6} M medroxyprogesterone-17-acetate (MPA) for 0–6 days to induce decidualization in vitro. RNA was extracted from ESCs at 0, 2, 4, and 6 days for qRT-PCR analysis. β-actin served as the internal control.

Animal experiments

All animal protocols were approved by the Ethics Committee of the Fourth Affiliated Hospital of Jiangsu University (2022006) and adhered to ethical requirements. We have complied with all relevant ethical regulations for animal use. An in vivo embryo implantation study was conducted as previously described with modifications[36]. Female ICR (Institute of Cancer Research) mice in estrus, aged 6–8 weeks, were mated with male ICR mice aged 8–10 weeks. All mice were purchased from the Animal feeding Center of Jiangsu University and were accompanied by quarantine certificates. ICR mice do not involve further processing such as genetic modification. The day of the vaginal plug observation was considered day 1 of pregnancy. On Day 3, pregnant mice were anesthetized at 09:00 a.m. and injected with 10 μL of a solution containing 1 μg of si-S100P into the right uterine horn, while 10 μL of a solution containing 1 μg of si-NC was injected into the left horn. Mice were dissected on Day 7 of pregnancy to assess embryo

implantation rates, and samples of the uterine endometrium were collected for IHC analysis.

Statistical analysis reproducibility

The data are presented as the means ± SEMs of at least three independent experiments. Each experiment was independently repeated three times, beginning with the cell treatment step. Analyses were performed using GraphPad Prism statistical software (version 9.0, GraphPad). After the assumption of a normal distribution was evaluated with the Kolmogorov–Smirnov test, an unpaired t test and one-way ANOVA followed by the Student-*t* test were performed when appropriate. One-way analysis of variance (ANOVA) was used for comparisons of multiple groups. P value < 0.05 was considered statistically significant: $^{*}P < 0.05$, $^{**}P < 0.01$, $^{***}P < 0.001$, and $^{****}P < 0.0001$.

Reporting summary

Further information on research design is available in the Nature Portfolio Reporting Summary linked to this article.

Data availability

Source data can be found in Supplementary Data. The uncropped blot images for figures in the text are available in Figure. S6.

Received: 27 May 2024; Accepted: 11 February 2025;
Published online: 26 February 2025

References

1. Sun, Y. et al. Prednisone vs Placebo and Live Birth in Patients With Recurrent Implantation Failure Undergoing In Vitro Fertilization. *JAMA* **329**, 1460–1468 (2023).
2. Achache, H. & Revel, A. Endometrial receptivity markers, the journey to successful embryo implantation. *Hum. Reprod. Update* **12**, 731–746 (2006).
3. Lai, Z.-Z. et al. Single-cell transcriptome profiling of the human endometrium of patients with recurrent implantation failure. *Theranostics* **12**, 6527–6547 (2022).
4. Lessey, B. A. Assessment of endometrial receptivity. *Fertil. Steril.* **96**, 522–529 (2011).
5. Shekibi, M., Heng, S. & Nie, G. MicroRNAs in the regulation of endometrial receptivity for embryo implantation. *Int. J. Mol. Sci.* **23**, 6210 (2022).
6. Craciunas, L. et al. Conventional and modern markers of endometrial receptivity: a systematic review and meta-analysis. *Hum. Reprod. Update* **25**, 202–223 (2019).
7. Kim, A., Jung, H., Choi, W. J., Hong, S. N. & Kim, H. Y. Detection of endometrial and subendometrial vasculature on the day of embryo transfer and prediction of pregnancy during fresh in vitro fertilization cycles. *Taiwan. J. Obstet. Gynecol.* **53**, 360–365 (2014).
8. Lessey, B. A. & Young, S. L. What exactly is endometrial receptivity? *Fertil. Steril.* **111**, 611–617 (2019).
9. Tempest, N. et al. Anterior Gradient Protein 3 and S100 Calcium-Binding Protein P Levels in Different Endometrial Epithelial Compartments May Play an Important Role in Recurrent Pregnancy Failure. *Int J. Mol. Sci.* **22**, 3835 (2021).
10. Mikolajczyk, M., Wirstlein, P. & Skrzypczak, J. The impact of leukemia inhibitory factor in uterine flushing on the reproductive potential of infertile women-a prospective study. *Am. J. Reprod. Immunol.* **58**, 65–74 (2007).
11. Sztachelska, M. et al. Oxytocin antagonism reverses the effects of high oestrogen levels and oxytocin on decidualization and cyclooxygenase activity in endometrial tissues. *Reprod. Biomed. Online* **39**, 737–744 (2019).
12. Bi, Y. et al. HOXA10 improves endometrial receptivity by upregulating E-cadherin. *†. Biol. Reprod.* **106**, 992–999 (2022).
13. Salmasi, S., Sharifi, M. & Rashidi, B. Ovarian stimulation and exogenous progesterone affect the endometrial miR-16-5p, VEGF protein expression, and angiogenesis. *Microvasc. Res* **133**, 104074 (2021).
14. Germeyer, A., Savaris, R. F., Jauckus, J. & Lessey, B. Endometrial beta3 Integrin profile reflects endometrial receptivity defects in women with unexplained recurrent pregnancy loss. *Reprod. Biol. Endocrinol.* **12**, 53 (2014).
15. Matsui, M. & Corey, D. R. Perspectives: Noncoding RNAs as drug targets. *Nat. Rev. Drug Discov.* **16**, 167 (2017).
16. Feng, C. et al. Construction of implantation failure related lncRNA-mRNA network and identification of lncRNA biomarkers for predicting endometrial receptivity. *Int. J. Biol. Sci.* **14**, 1361–1377 (2018).
17. Zeng, H., Fan, X. & Liu, N. Expression of H19 imprinted gene in patients with repeated implantation failure during the window of implantation. *Arch. Gynecol. Obstet.* **296**, 835–839 (2017).
18. Li, J. et al. Increased new lncRNA-mRNA gene pair levels in human cumulus cells correlate with oocyte maturation and embryo development. *Reprod. Sci.* **22**, 1008–1014 (2015).
19. Wang, Y. et al. A novel molecule in human cyclic endometrium: LncRNA TUNAR Is involved in embryo implantation. *Front Physiol.* **11**, 587448 (2020).
20. Suhorutshenko, M. et al. Endometrial receptivity revisited: endometrial transcriptome adjusted for tissue cellular heterogeneity. *Hum. Reprod.* **33**, 2074–2086 (2018).
21. Xing, C., Sun, S., Yue, Z.-Q. & Bai, F. Role of lncRNA LUCAT1 in cancer. *Biomed. Pharmacother.* **134**, 111158 (2021).
22. Chi, J. et al. Long non-coding RNA LUCAT1 promotes proliferation and invasion in gastric cancer by regulating miR-134-5p/YWHAZ axis. *Biomed. Pharmacother.* **118**, 109201 (2019).
23. Jiao, Y., Li, Y., Ji, B., Cai, H. & Liu, Y. Clinical Value of lncRNA LUCAT1 Expression in Liver Cancer and its Potential Pathways. *J. Gastrointest. Liver Dis.* **28**, 439–447 (2019).
24. Zhou, Q. et al. LUCAT1 promotes colorectal cancer tumorigenesis by targeting the ribosomal protein L40-MDM2-p53 pathway through binding with UBA52. *Cancer Sci.* **110**, 1194–1207 (2019).
25. Prica, F., Radon, T., Cheng, Y. & Crnogorac-Jurcevic, T. The life and works of S100P - from conception to cancer. *Am. J. Cancer Res* **6**, 562–576 (2016).
26. Tao, Y. et al. Long noncoding RNA LUCAT1 enhances the survival and therapeutic effects of mesenchymal stromal cells post-myocardial infarction. *Mol. Ther. Nucleic Acids* **27**, 412–426 (2022).
27. Huan, L. et al. Hypoxia induced LUCAT1/PTBP1 axis modulates cancer cell viability and chemotherapy response. *Mol. Cancer* **19**, 11 (2020).
28. Nai, Y., Pan, C., Hu, X. & Ma, Y. LncRNA LUCAT1 contributes to cell proliferation and migration in human pancreatic ductal adenocarcinoma via sponging miR-539. *Cancer Med* **9**, 757–767 (2019).
29. Liu, C., Moten, A., Ma, Z. & Lin, H.-K. The foundational framework of tumors: gametogenesis, p53, and cancer. *Semin Cancer Biol.* **81**, 193–205 (2022).
30. Liao, K. et al. The LGMN pseudogene promotes tumor progression by acting as a miR-495-3p sponge in glioblastoma. *Cancer Lett.* **490**, 111–123 (2020).
31. MicroRNA-495-3p functions as a tumor suppressor by regulating multiple epigenetic modifiers in gastric carcinogenesis - Eun - 2018 - The Journal of Pathology - Wiley Online Library. https://pathsocjournals.onlinelibrary.wiley.com/doi/10.1002/path.4994.
32. Arumugam, T., Simeone, D. M., Schmidt, A. M. & Logsdon, C. D. S100P stimulates cell proliferation and survival via receptor for activated glycation end products (RAGE). *J. Biol. Chem.* **279**, 5059–5065 (2004).

33. Arumugam, T., Ramachandran, V., Gomez, S. B., Schmidt, A. M. & Logsdon, C. D. S100P-derived RAGE antagonistic peptide reduces tumor growth and metastasis. *Clin. Cancer Res* **18**, 4356–4364 (2012).
34. Mercado-Pimentel, M. E. et al. The S100P/RAGE signaling pathway regulates expression of microRNA-21 in colon cancer cells. *FEBS Lett.* **589**, 2388–2393 (2015).
35. Onyeagucha, B. C., Mercado-Pimentel, M. E., Hutchison, J., Flemington, E. K. & Nelson, M. A. S100P/RAGE signaling regulates microRNA-155 expression via AP-1 activation in colon cancer. *Exp. Cell Res.* **319**, 2081–2090 (2013).
36. Akbar, R. et al. miR-183-5p regulates uterine receptivity and enhances embryo implantation. *J. Mol. Endocrinol.* **64**, 43–52 (2020).

Acknowledgements

This research was supported by grants from the National Natural Science Foundation of China (Grant No. 82172838), the 333 Project Excellent Young Talents Project of Jiangsu Province, the Natural Science Foundation of Jiangsu Province (Grant No. BK20241860), and the Key Medical Research Projects of Jiangsu Provincial Health Commission (Grant No. K2023078).

Author contributions

X.Z. designed this study. X.Z., L.L. and Y.L. obtained funding. J.S., Y.C., L.L., J.X., M.Z., S.Z., J.L. and X.S. performed the clinical studies. J.S., Y.C., Q.J., W.L., M.L., J.S., and J.Z. performed the experiments. J.S., Y.C., Q.J., and W.L. performed the statistical analyses. J.S. wrote the manuscript. X.Z. revised the manuscript. All the authors read, revised, and approved the final manuscript.

Competing interests

The authors declare no competing interests.

Ethical approval and consent to participate

The study was approved by the Ethics Committee of the Fourth Affiliated Hospital of Jiangsu University. Written informed consent was obtained from all participants.

Additional information

Supplementary information The online version contains supplementary material available at https://doi.org/10.1038/s42003-025-07718-4.

Correspondence and requests for materials should be addressed to Xiaolan Zhu.

Peer review information : *Communications Biology* thanks the anonymous reviewers for their contribution to the peer review of this work. Primary Handling Editor: Christina Karlsson Rosenthal